

# Investigation of the Systematic Time Mark Shift for the Signals from the Organic Scintillator Based Neutron Spectrometer

Prusachenko P., Khryachkov V., Bobrovsky T., Ketlerov V., Bondarenko I.

*Institute for Physics and Power Engineering, Obninsk, Russia*

## 1. Introduction

Organic scintillators are widely used for fast neutron spectrometry. In most cases, the time-of-flight method is used. The accuracy of the neutron energy measurement depends on the accuracy of time mark determination. This is especially important for performing experiments on the measurement of the prompt fission neutron spectra, which are characterized by a rapid change in the neutron yield depending on their energy. Even the small shift in the time mark definition can lead to a serious error in determining the yields of fission neutrons [1]. It is usually in experimental practice that the correction to the time mark shift is determined only for events caused by the detection of gamma rays. Then this correction is applied to correct the time mark of both signals from neutrons and gamma rays [2–7]. The purpose of this work was to study the possible systematic time mark shifts for signals caused by the detection of both neutrons and gamma rays in an organic scintillator. Analysis of the time mark position was performed using the most widely used algorithms – software emulation of the constant-fraction discriminator and the leading edge discriminator. The comparison of the obtained results was made, depending on the algorithm used and its input parameters.

## 2. Experimental setup

The time mark position can be obtained by analyzing the time distributions corresponding to events with the fixed detection time. Using the signal area and the time-of-flight values, this analysis can be performed depending on the signal amplitude. In our case, we analyzed the prompt neutrons and gamma rays from the  $D(d,n)^3\text{He}$  reaction. The neutron detector was located in a special massive shielding at the 0 degrees angle relative to the ion beam axis. Both signals, the signal from the pick-up electrode of the accelerator chop-buncher system and the signal from the neutron detector were simultaneously digitized and stored on the disk for further processing. The main parameters of the experiment are shown in Table 1. The experimental setup is shown in Fig. 1.

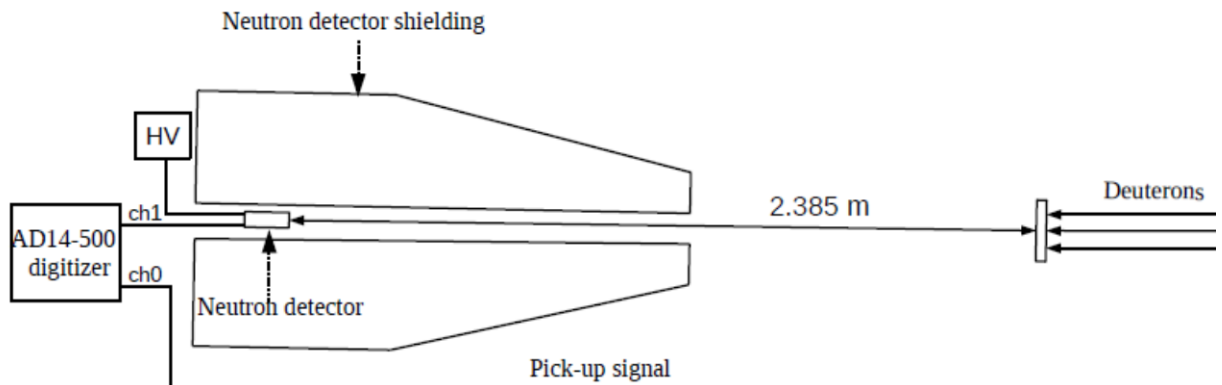


Fig. 1. Experimental setup.

Table 1. The main parameters of experimental setup.

Accelerator operation mode	Pulse mode, pulse width ~1.2 ns.
Accelerated ions type	deutrons
Ion energy	5.952 MeV
Average neutron energy (0 deg.)	9.112±0.005 MeV
Target	D-Ti, 1275±50 ug/cm <sup>2</sup>
Neutron detector	Stilbene, 40×40 mm PMT ET Enterpize 9813QB
Flight path	237.7±0.2 cm
Data acquisition system	AD14-500 waveform digitizer 500 MSamples per second 14 bit ADC resolution.

### 3. Digital Signal Processing

#### 3.1 $n/\gamma$ separation

To determine the type of particle that caused the event in the detector, correlation analysis of signals was used [8, 9]. The signal from gamma rays averaged over 5000 events was used as the target signal for the correlation function calculation. The separation quality obtained for the entire range of the pulse areas is shown in Fig. 2. The dynamic threshold on the separation parameter was used for selection events from neutrons and gamma rays [9].

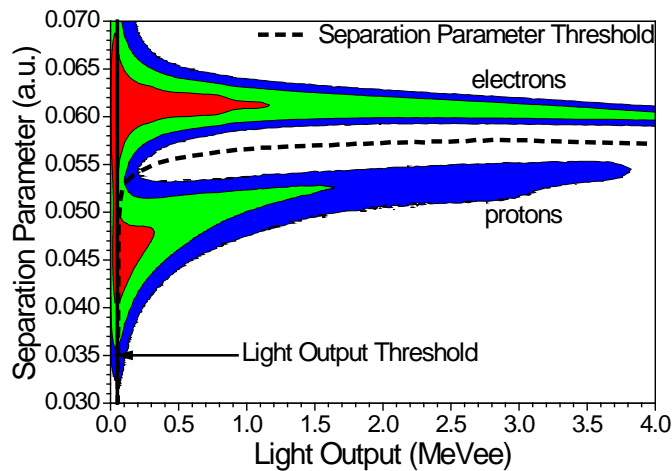


Fig. 2. Two-dimensional spectrum, the separation parameter vs. pulse area. Dotted line – the threshold for the separation parameter.

### 3.2 Time Mark Definition

The study of the systematic errors was carried out for the two most used algorithms for the time mark definition - algorithms that emulate the operation of the constant-fraction discriminator (CFD) and the leading edge discriminator (LED).

In the case of the constant-fraction discriminator algorithm, the operation of the classical CF discriminator was emulated [5, 10]. The time of the baseline crossing of the bipolar pulse formed by summing the main signal, delayed in time, and its copy, inverted and attenuated in 5 times, was used as the time mark (Fig. 3). The accurate time of the baseline crossing was determined by approximating three points near the zero by the parabola. A study of the time mark behavior was conducted for several values of the main signal delay: 8 (CFD # 1), 12 (CFD # 2) and 20 ns (CFD # 3). For the delays above and below these values, the time resolution deteriorated sharply.

The use of the leading-edge discriminator algorithms is associated with a strong amplitude dependence of the time mark position. In our work, we applied an improved algorithm. The time point when the signal reached the predetermined fraction of its pulse height was used as the time mark (Fig. 4). The accurate value of this time point was determined by linear interpolation. The algorithm was compared for several fraction values: 10 (LE#1), 25 (LE#2), and 50% (LE#3) of the pulse height.

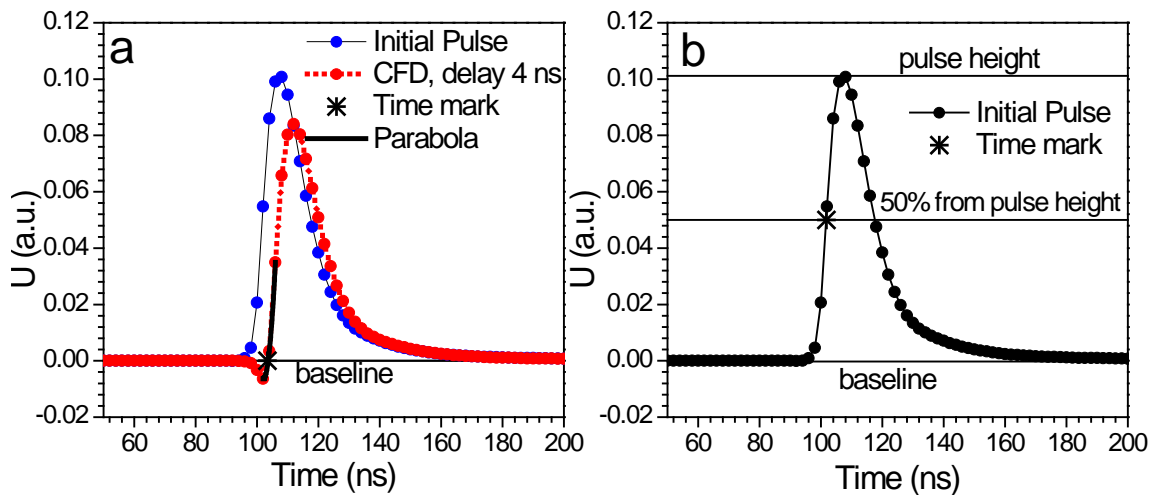


Fig. 3. Demonstration of digital algorithms CFD and LED.

### 4. Time distribution analysis

After the events selection on the separation parameter, time distributions were constructed for both gamma rays and neutrons. In both distributions, narrow peaks are observed, corresponding to the detection of prompt gamma rays and neutrons emitted from the target (Fig. 4).

The main contribution in the background for gamma rays time distribution was made the scattering on the accelerator target node and the random coincidences background, which practically not influenced on the distribution form (Fig. 5). The scattered neutron contribution in the neutrons time spectrum was more significant (Figs. 5, 6). The small amount of the high-energy neutrons was observed to the left of the main peak (Figs. 5, 6).

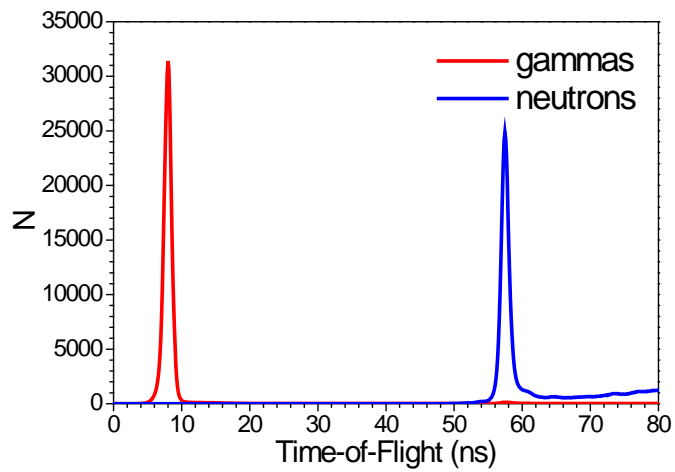


Fig. 4. The time distributions for gamma-rays and neutrons.

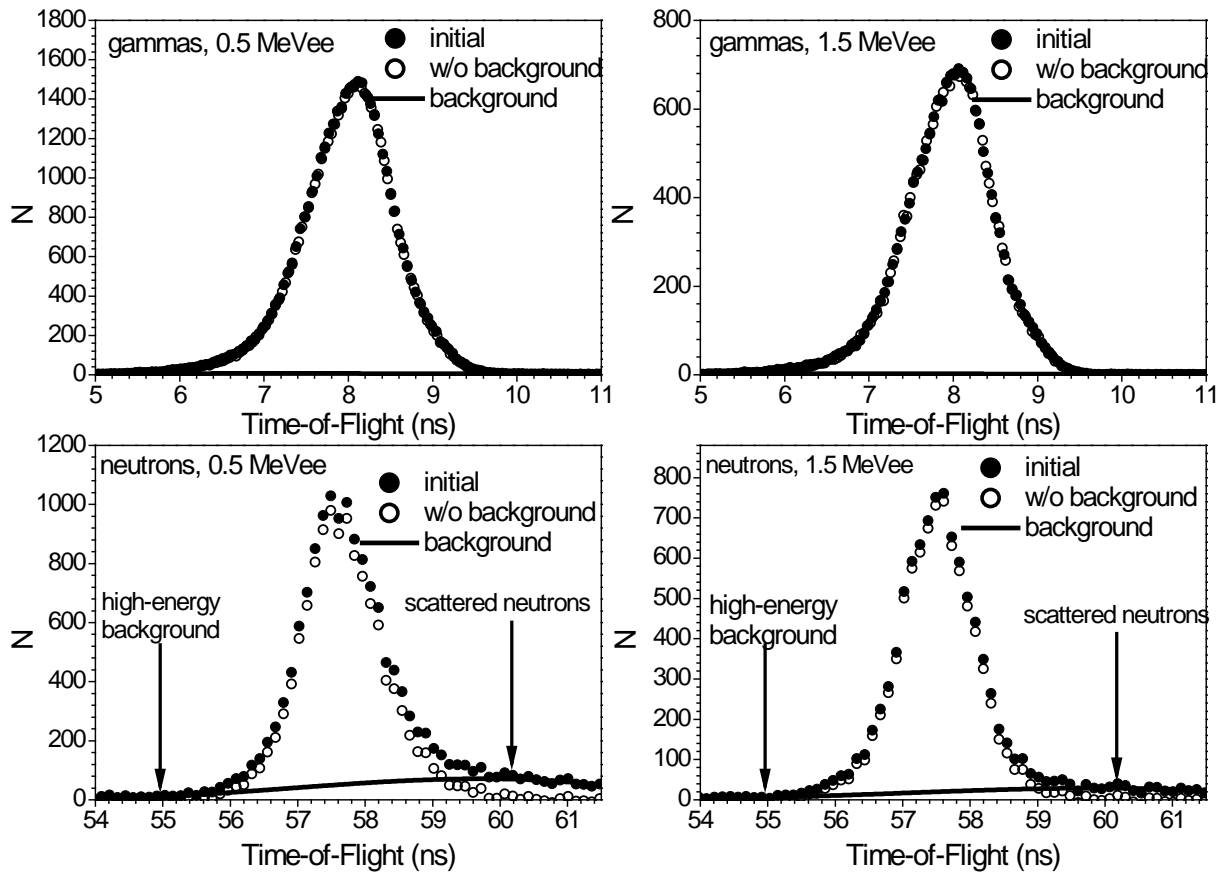


Fig. 5. The time distribution of gamma and neutron for the several fixed pulse area values.

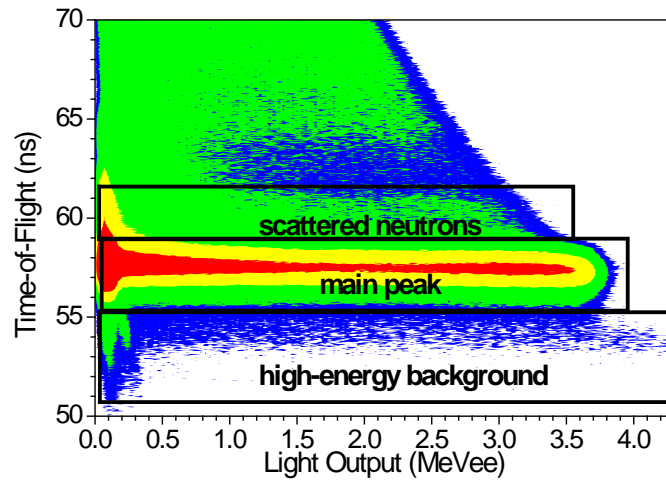


Fig. 6. The neutron two-dimensional spectrum – light output vs. time-of-flight.

The amplitude dependence of the time mark shift was determined by analyzing the position of the peaks of prompt gamma rays and neutrons for the different fixed pulse area values. The value of the peak's mathematical expectation after subtracting the background (Fig. 5) was taken as the estimation the peak position. In the gamma rays case, the average peak position  $M_{\gamma av}$  was calculated after the definition of the position of the prompt gamma rays peak for all values of the pulse area. The time mark shift for the fixed value of the pulse area  $\Delta t_{\gamma i}$  was determined as the difference between the peak position for this pulse area  $M_{\gamma i}$  and the average position of the prompt gamma rays peak for the all range of the pulse areas  $M_{\gamma av}$ :

$$\Delta t_{\gamma i} = M_{\gamma i} - M_{\gamma av} \quad (1)$$

In the neutron case, we determined the time mark shift for the fixed value of the pulse area  $\Delta t_{ni}$  as the difference between the expected neutron time-of-flight  $ToF_{ne}$  and the experimental value of the neutron time-of-flight for this pulse area value  $ToF_{ni}$ :

$$\Delta t_{ni} = ToF_{ne} - ToF_{ni} \quad (2)$$

The experimental time-of-flight value  $ToF_{ni}$  for the fixed pulse area was calculated using follow equation:

$$ToF_{ni} = M_{ni} - M_{\gamma av} + 3.335641d \quad (3)$$

where  $M_{ni}$  – mathematical expectation of neutron peak for fixed pulse area  $i$ ,  $M_{\gamma av}$  – the average position of the prompt gamma peak,  $d$  – the flight path in meters. The expected neutron time-of-flight value  $ToF_{ne}$  was calculated using the known value of the average neutron energy and the known flight path:

$$ToF_{ne} = 3.335641d \frac{E+A}{\sqrt{E(E+2A)}} \quad (4)$$

where  $A$  – neutron mass (939.565 MeV),  $E$  – neutron energy in MeV,  $d$  – flight path in meters.

## 5. Results of time distribution analysis

The results of the time distributions analysis are shown in Fig. 7. For all cases considered, the neutron peak centroids are systematically shifted relative to the expected value, calculated from the known neutron energy and the known flight path. The value of the systematic shift depends on the algorithm's type, its parameters and the pulse area. This indicates that the time mark definition using the most commonly used algorithms can lead to its systematic shift, and therefore to a shift in the neutron energy definition. For the CFD algorithm with the increase of the delay and for the LED algorithm with the increase of the threshold fraction, the value of the observed shift increases.

An analysis of the experimental results showed that for all the analyzed cases the shape of the curve for neutrons differs from that for gamma rays. The dependence of the peak centroid position on the pulse area is also observed for gamma rays, which also can be seen in the other author's works [2–7]. It can also be noted that the time mark quality obtained using the modified LED algorithm is insignificantly worse than that of the CFD algorithm.

The observed time mark position shift for neutrons and its difference from that for gamma rays can be explained by the difference in the pulse shapes from neutrons and gamma rays. In this case, it should be observed both for digital algorithms and when using analog electronics.

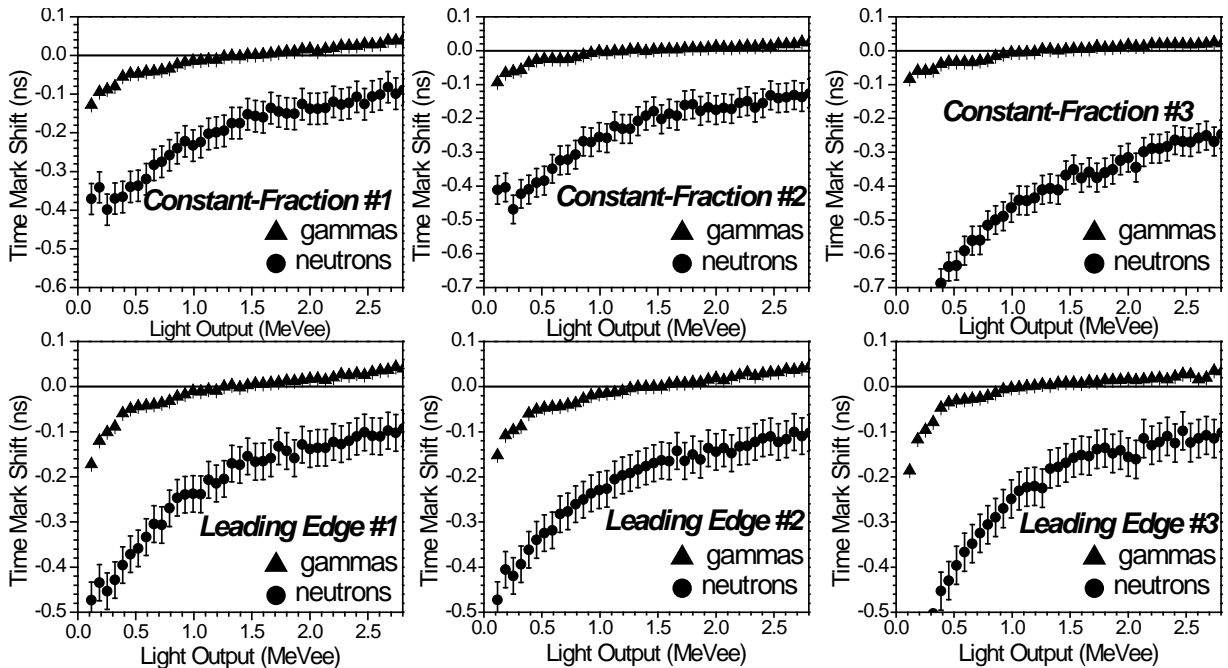


Fig. 7. The time mark shift for neutrons and gamma rays as the pulse area function. The results are given for all algorithms considered in the work.

## 6. Influence on the neutron spectrum measurements

The shift in the detected neutron energy will depend on the flight path. The larger the flight path, the smaller the error in determining the energy. Fig. 8 shows the energy dependence of the systematic shift in the neutron energy for the extreme cases considered in the work (CFD#1,3, LE#1,3). The value of the shift is given at the flight path of 1 meter. For large values of the flight path (more than 2.5–3 meters) the shift value will be negligible. Also, from the results it can be seen that the time mark shift will have the greatest influence at neutron energies above 6 MeV.

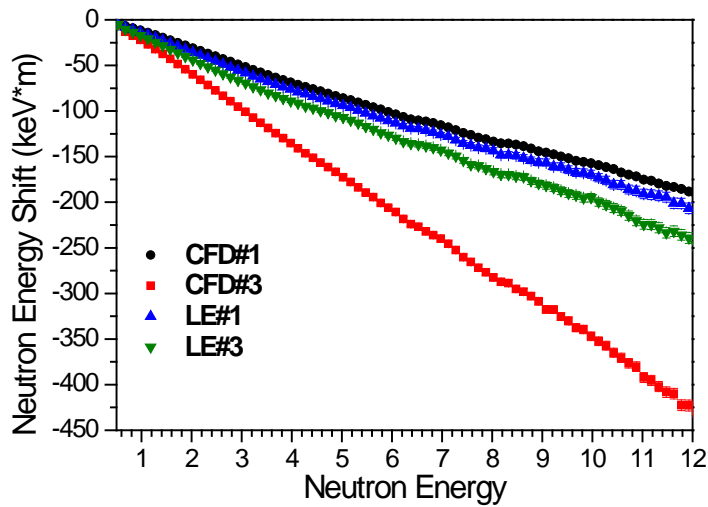


Fig. 8. The shift in the neutron energy definition as the neutron energy function for several algorithms.

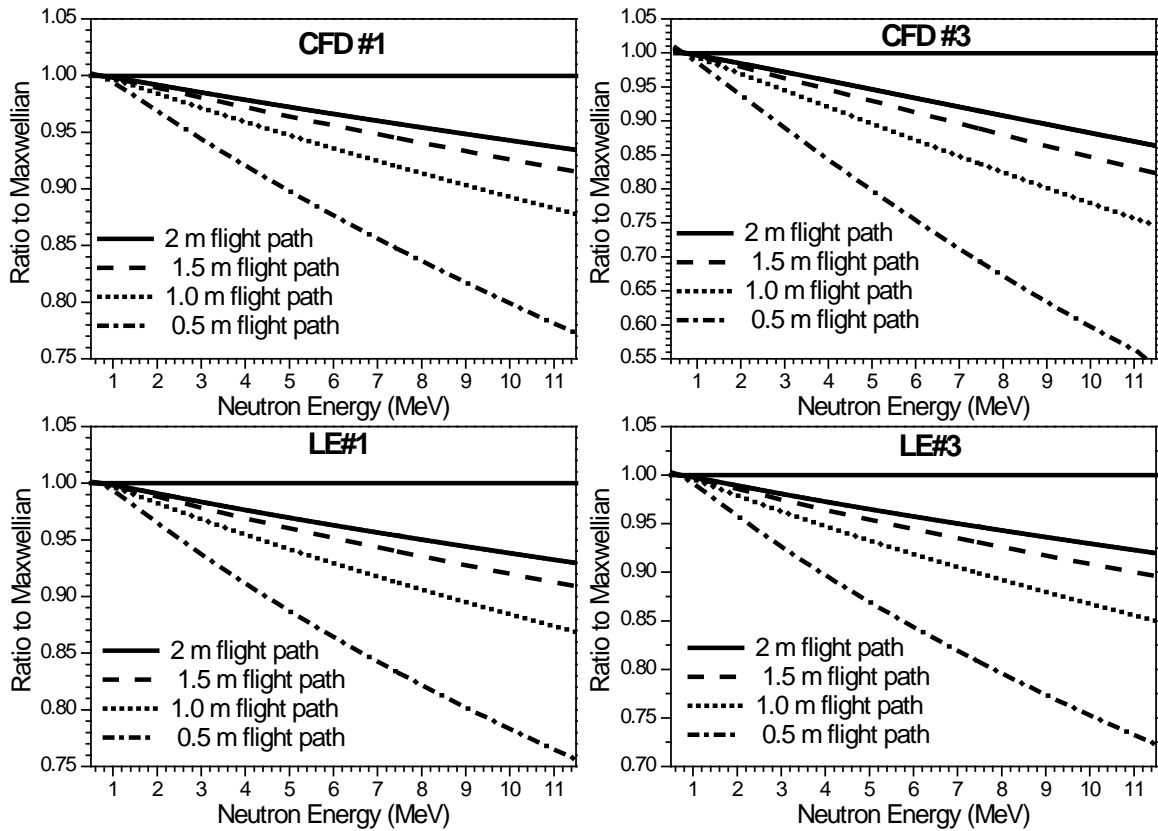


Fig. 9. The demonstration of the time mark shift influence on the prompt neutron yield measurements.

The prompt fission neutron spectra are characterized by a sharp change in the neutron yield with an increase in their energy. Therefore, even a small error in the determination of energy can lead to a serious error in determining the yield of fission neutrons. Fig. 9 shows the possible influence of the time mark shift on the measurements of the prompt fission neutron yield as the neutron energy function. The results were obtained by simulating the  $^{252}\text{Cf}$

prompt neutron spectrum (the Maxwell distribution with  $T=1.42$  MeV) using the neutron energy shift data (Fig. 8) for the different algorithms and flight path values.

It should be noted that most measurements of the prompt fission neutron spectra are carried out on the short flight path (0.5–2 m), so the observed effect can have a significant impact on the results of measurements of fission neutron yields at different energies. In turn, this may lead to an error in determining the average energy of the fission neutrons spectrum.

## 7. Conclusions

The analysis of systematic shifts in the time mark definition was carried out for the digital algorithms that emulate the operation of the constant-fraction discriminator and the leading edge discriminator. The influence of the algorithms input parameters of the shift value is studied.

For all cases considered, the neutron peak centroids are systematically shifted relative to the expected value, calculated from the known neutron energy and the known flight path. The value of the systematic shift depends on the algorithm's type, its parameters and the pulse area. For the CFD algorithm with the increase of the delay and for the LED algorithm with the increase of the threshold fraction from the signal pulse height, the value of the observed shift increases.

An analysis of the experimental results showed that for all the analyzed cases the shape of the curve for neutrons differs from that for gamma rays. Therefore, it is incorrect to use as a correction for the neutron signals the time mark shift value determined from the analysis of the prompt gamma rays peak. The correction for the time mark of the neutron signals must be determined separately.

It is shown that the observed systematic time mark shift for signals from neutrons will lead to a significant shift in the neutron energy value determined from their time-of-flight for short flight path (less than 2 meters). This is especially critical for experiments on the prompt fission neutron spectra measurements, since they are characterized by a rapid change in neutron yield with an increase in their energy. In turn, this may lead to an error in determining the average energy of the fission neutrons spectrum.

## References

1. R.C. Haight, H.Y. Lee, T.N. Taddeucci, et al., Nuclear Data Sheets **119** (2014) 205.
2. A.S. Vorobyev, O.A. Shcherbakov, Yu.S. Pleva et al., Nuclear Instruments and Methods in Physics Research A **598** (2009) 795.
3. E. Blain, A. Daskalakis, R. C. Block, et al., Physical Review C **95** (2017) 064615.
4. S. Noda, R. C. Haight, R. O. Nelson et al., Physical Review C **83** (2011) 034604.
5. A. Gook, F.-J. Hamsch, and M. Vidali, Physical Review C **90** (2014) 064611.
6. C. Matei, F.-J. Hamsch, S. Oberstedt, Nuclear Instruments and Methods in Physics Research A **676** (2012) 135.
7. N.V. Kornilov, I. Fabry, S. Oberstedt, F.-J. Hamsch, Nuclear Instruments and Methods in Physics Research A **599** (2009) 226
8. N.V. Kornilov, V.A. Khriatchkov, M. Dunaev, et al., Nuclear Instruments and Methods in Physics Research A **497** (2003) 467.
9. P.S. Prusachenko, V.A. Khryachkov, V.V. Ketlerov, et al., Nuclear Instruments and Methods in Physics Research A **905** (2018) 160.
10. Rudlevski P.D., Khriachkov V.A., Dunaev M.V., Proceeding of XII International Seminar on Interaction of neutrons with Nuclei (2004), 415.